

Multi-Attention Multiple Instance Learning

Andrei V. Konstantinov and Lev V. Utkin
 Peter the Great St.Petersburg Polytechnic University
 St.Petersburg, Russia
 e-mail: andrue.konst@gmail.com, lev.utkin@gmail.com

Abstract

A new multi-attention based method for solving the MIL problem (MAMIL), which takes into account the neighboring patches or instances of each analyzed patch in a bag, is proposed. In the method, one of the attention modules takes into account adjacent patches or instances, several attention modules are used to get a diverse feature representation of patches, and one attention module is used to unite different feature representations to provide an accurate classification of each patch (instance) and the whole bag. Due to MAMIL, a combined representation of patches and their neighbors in the form of embeddings of a small dimensionality for simple classification is realized. Moreover, different types of patches are efficiently processed, and a diverse feature representation of patches in a bag by using several attention modules is implemented. A simple approach for explaining the classification predictions of patches is proposed. Numerical experiments with various datasets illustrate the proposed method.

Keywords: Multiple instance learning, attention mechanism, classification, explanation

1 Introduction

The Multiple Instance Learning (MIL) as a type of weakly supervised learning is a framework which is applied to many applications, including the drug activity prediction [1], detecting the lung cancer [2], the protein function annotation [3], histology [4, 5, 6], and many others. The corresponding survey works describing various MIL problem statements and applications can be found in [7, 8, 9, 10, 11, 12, 13].

In contrast to traditional machine learning models, MIL deals with a set of bags that are labeled such that each bag consists of many unlabeled instances, i.e. instances in the bags have no label information, and we have weakly annotated data. MIL aims to train a classifier that assign labels to testing bags or to assign labels to unlabeled instances in bags. The standard MIL assumption states that all negative bags contain only negative instances, and that positive bags contain at least one positive instance. It is important that this is one of the possible MIL problem statements. Other statements are when, for example, instances are annotated by an expert or when instances as well as bags do not have labels [14].

Many MIL models which adapt various conventional models to solving MIL tasks have been proposed in literature, for example, the KNN is adapted to the citation-kNN [15], the SVM to mi-SVM and MI-SVM [16], decision trees to ID3-MI [17], convolutional neural networks to the Multiple Instance Learning Convolutional Neural Network [18, 19, 20].

One of the promising approaches to improve the MIL models is to use the attention mechanism. An attention-based MIL was proposed in [21] where the linear regression model was replaced by a one-layer neural network with single output. Following this work, several methods of MIL based on the attention mechanism have been developed, including Deep Attention Multiple Instance Survival Learning [12], ProtoMIL [22], MHAttnSurv [23], the loss-attention MIL [24], MILL [25]. There are other MIL methods using the attention mechanism, which can be found in [26, 27, 28]. An interesting method for applying attention

to the MIL problem is provided by Ilse et al. [29]. We will use this method as a basic attention-based approach to MIL and call it as AbDMIL (Attention-based Deep Multiple Instance Learning) below.

However, the above methods have some disadvantages. First of all, they do not take into account the neighboring patches or instances which may significantly impact on a prediction especially when images are considered as bags. Our experiments show that neighbors can be regarded as an additional information about a patch. That is why we propose to analyze every patch jointly with K neighbors where K can be viewed as a tuning parameter. Moreover, we propose to transform all neighbors to a single embedding which collects all information from neighbors into one vector. This is implemented by means of the attention. In order to simplify the analysis, we consider only adjacent patches because they are the most informative. Another important advantage of taking into account neighbors is that patches can be selected as small as possible because each patch jointly with neighbors can cover an increased area of the whole image. Smaller patches have simpler procedures for their processing. The larger the size of a patch, the less the possibility of interpreting the result (in the extreme case, the patch is the whole image), and also the more difficult the task of training the model under condition of small sizes of the training instances. In general case, if we assume that instances of a bag impact on a bag label jointly with their neighbors, then the classification problem could be reformulated in terms of the standard MIL problem statement. For example, we could form new enlarged instances consisting of the initial instances with neighbors. However, the order of neighbors in this case will be taken into account. This property is not desirable. Another difficulty is variability of neighbors number which may take place in many applications, for example, in computational histopathology. Moreover, if we apply a MIL algorithm to new instances in this case, then identical parts of different new instances will be performed differently. In order to overcome this disadvantage, we propose to apply an encoder network to every instance and to compose joint embeddings of instances with neighbors.

Second, most MIL methods use the attention mechanism under condition that attention weights allow us to find key instances in the whole image. This application of the attention is very important because its use enhances the classification quality. However, the attention can be used in a more wide sense. We introduce the multiple attention mechanism which is based on training a set of templates. The templates may be very useful when patches or instances corresponding to a positive label are significantly different. Each template and the corresponding attention is responsible for every type of patches. The templates are viewed as trainable parameters which are trained under condition that they should be different in order to take into account different aspects of instances. Another peculiarity of the proposed scheme is that we avoid the concatenation operation with embeddings obtained by means of the attention modules. In other words, we propose to aggregate embeddings of templates by using the attention mechanism instead of the direct use of a neural network to a set of concatenated embeddings. An additional attention is used to processing all these embeddings. As a result, we do not need to train the encoder neural network on every new type of patches. It is trained once, and only templates are trained for new patches.

In sum, we propose a multiple attention scheme for solving the MIL problem called MAMIL, where one of the attention modules takes into account adjacent patches or instances (Neighborhood attention), several attention modules (Template Attentions) are used to get a diverse feature representation of each patch, and one attention (Final Attention) is used to unite different feature representations and to classify each patch (instance) and the whole bag.

Our contributions can be summarized as follows:

1. A new MIL model, which takes into account the neighboring patches or instances of each analyzed patch.
2. A way to join all information available in neighbors of a patch in the form of a united embedding by means of the neighborhood attention, which takes into account the proximity of each neighbor to the corresponding patch.
3. A way to efficiently process different types of patches and to implement diverse feature representation of patches in a bag by using several attention modules.

4. A combined representation of patches and their neighbors in the form of an embedding of a small dimensionality for simple classification.
5. Explaining why a patch is classified in a certain way.

Numerical experiments with various datasets illustrate the proposed method. In particular, four datasets constructed from the well-known MNIST dataset [30] to get the specific MIL datasets are studied. Five datasets Musk1, Musk2 [1], Fox, Tiger, Elephant [16] with numerical features are used to perform tabular data. Since one of the important applied areas, where MIL can be viewed as a main and inherent tool, is the computational histopathology, then we study the proposed method by using the Breast Cancer Cell Segmentation dataset [31] consisting of histopathology images.

The paper is organized as follows. Related work can be found in Section 2. A brief introduction to MIL and basics of the attention mechanism are given in Section 3. The proposed method and the corresponding general scheme are provided in Section 4. Computing the instance importance for the explanation purposes is considered in Section 5. A brief discussion of introduced template properties can be found in Section 6. Numerical experiments are provided in Section 7. Concluding remarks can be found in Section 8.

2 Related work

MIL. Many models have been proposed to modify various machine learning methods for solving the MIL problem, including the citation-kNN [15], the mi-SVM and MI-SVM [16], the ID3-MI [17]. MIL models using ensemble-based approaches, for example, AdaBoost, Random Forest, etc., were developed and presented in [32, 33, 34]. A comparison of some ensemble-based MIL models can be found in [35].

The large importance of MIL in many applications motivated developing models based on neural networks and convolutional neural network [36, 18, 19, 20]. We can also point out such models as MI-BDNN [37], Deep MIML [38], MI-ELM [39].

Elements of the explanation methods [40, 41, 42, 43] were used to provide interpretability of the MIL models [22].

A huge amount of methods and models were developed to apply MIL to the computational histopathology where histology images can be viewed as bags and are often represented as a set of small parts (patches, cells) which can be referred to as “instances”. Many survey papers [4, 5, 11, 14] study various aspects of the computational histopathology as a MIL problem.

Various deep learning MIL models provide an important opportunity to improve accuracy of the MIL predictions, to correctly classify bags as well as their instances. However, a more interesting approach based on applying the attention mechanism to solving the MIL problem opens another direction in development of the accurate classification methods of MIL.

MIL and attention. In spite of a few papers devoted to application of the attention mechanism [44, 45] to solving the MIL problem, it can be regarded as a promising approach to improve the MIL models. Starting from the attention-based MIL [21] and following this work, several interesting models using the attention mechanism have been developed. They, for example, include DeepAttnMISL (Deep Attention Multiple Instance Survival Learning) [12], MHAttnSurv (Multi-Head Attention for Survival Prediction) [23], ProtoMIL (Multiple Instance Learning with Prototypical Parts) [22], SA-AbMILP (Self-Attention Attention-based MIL Pooling) [46], the loss-attention MIL (the instance weights are calculated based on the loss function) [24], DSMIL (Dual-stream Multiple Instance Learning) [27] MILL (Multiple Instance Learning-based Landslide classification) [25], AbDMIL [29]. There are other MIL methods using the attention mechanism, which can be found in [26, 47, 28]. The aforementioned methods propose approaches to enhance the MIL classification quality by using the attention. However, they do not take into account neighboring patches of each analyzed patch and do not propose to aggregate information which can be elicited from the neighborhood. In contrast to these methods, the proposed MAMIL provides an attention-based way for aggregating and incorporating the neighbors into the general MIL. MAMIL provides a flexible

diverse representation of a bag structure in the form of templates which allow us to consider different aspects of instances and to take into account new types of patches by training only attention models.

3 Preliminary

3.1 Multiple Instance Learning

According to the MIL problem statement, bags have class labels, but instances are unlabeled. This is the weakly supervised learning problem. The lack of labels for instances is a key peculiarity of MIL which motivates to solve two tasks. The first one is to annotate instances of bags. The second task is to classify new bags. In order to solve the tasks, we have to define conditions which connect the instance labels and the bag classes. Let X be a bag defined as a set of feature vectors $X = \{\mathbf{x}_1, \dots, \mathbf{x}_m\}$. Each instance is represented as feature vector \mathbf{x}_i in feature space \mathcal{X} . It can be mapped to a class by some function $f : \mathcal{X} \rightarrow \{0, 1\}$, where the negative and positive classes denoted as y_1, \dots, y_m correspond to 0 and 1, respectively. Classes y_1, \dots, y_m remain unknown during training. It should point out that binary classes is a special case of a general classification problem where the number of classes may be arbitrary. The number of instances m can also vary for different bags. We will denote bags by capitals and instances by bold letters.

Let us define conditions of the class label assignment to bags. The most common condition is that negative bags contain only negative instances, and positive bags contain at least one positive instance [9]. This implies that the bag classifier $g(X)$ is defined by

$$g(X) = \begin{cases} 1, & \exists \mathbf{x} \in X : f(\mathbf{x}) = 1, \\ 0, & \text{otherwise.} \end{cases} \quad (1)$$

Another more general condition is when a threshold θ is introduced to define the bag classifier $g(X)$, i.e., there holds

$$g(X) = \begin{cases} 1, & \theta \leq \sum_{\mathbf{x} \in X} f(\mathbf{x}), \\ 0, & \text{otherwise.} \end{cases} \quad (2)$$

The first condition can be regarded as a special case of the second one when $\theta = 1$. Only the first condition is used below.

3.2 Basics of the attention mechanism

The attention mechanism can be regarded as a tool by which a neural network can automatically distinguish the relative importance of features and weigh the features for enhancing the classification accuracy. It can be viewed as a learnable mask which emphasizes relevant information in a feature map. It is pointed out in [48, 45] that the original idea of attention can be understood from the statistics point of view applying the Nadaraya-Watson kernel regression model [49, 50]. Given n training instances $S = \{(\mathbf{x}_1, y_1), (\mathbf{x}_2, y_2), \dots, (\mathbf{x}_n, y_n)\}$, in which $\mathbf{x}_i = (x_{i1}, \dots, x_{id}) \in \mathbb{R}^d$ represents a feature vector involving d features and $y_i \in \mathbb{R}$ represents the regression outputs, the task of regression is to construct a regressor $f : \mathbb{R}^d \rightarrow \mathbb{R}$ which can predict the output value y of a new observation \mathbf{x} , using available training data S . The similar task can be formulated for the classification problem.

The original idea behind the attention mechanism is to replace the simple average of outputs $y^* = n^{-1} \sum_{i=1}^n y_i$ for estimating the regression output y corresponding to a new input feature vector \mathbf{x} with the weighted average in the form of the Nadaraya-Watson regression model [49, 50]:

$$y^* = \sum_{i=1}^n \alpha(\mathbf{x}, \mathbf{x}_i) y_i, \quad (3)$$

where weight $\alpha(\mathbf{x}, \mathbf{x}_i)$ conforms with relevance of the i -th training instance to the vector \mathbf{x} .

In other words, according to the Nadaraya-Watson regression model, to estimate the output y of an input variable \mathbf{x} , training outputs y_i given from a dataset weigh in agreement with the corresponding input \mathbf{x}_i locations relative to the input variable \mathbf{x} . The closer an input \mathbf{x}_i to the given variable \mathbf{x} , the greater the weight assigned to the output corresponding to \mathbf{x}_i .

One of the original forms of weights is defined by a kernel K (the Nadaraya-Watson kernel regression [49, 50]), which can be regarded as a scoring function estimating how vector \mathbf{x}_i is close to vector \mathbf{x} . The weight is written as follows [45]:

$$\alpha(\mathbf{x}, \mathbf{x}_i) = \frac{K(\mathbf{x}, \mathbf{x}_i)}{\sum_{j=1}^n K(\mathbf{x}, \mathbf{x}_j)}. \quad (4)$$

The above expression is an example of weights in nonparametric attention [45]. In terms of the attention mechanism [44], vector \mathbf{x} , vectors \mathbf{x}_i and outputs y_i are called as the query, keys and values, respectively. Weight $\alpha(\mathbf{x}, \mathbf{x}_i)$ is called as the attention weight. Therefore, the standard attention applications are often represented in terms of queries, keys and values, and the attention weights are expressed through these terms.

Generally, weights $\alpha(\mathbf{x}, \mathbf{x}_i)$ can be extended by incorporating learnable parameters. For example, if we denote $\mathbf{q} = \mathbf{W}_q \mathbf{x}$ and $\mathbf{k}_i = \mathbf{W}_k \mathbf{x}_i$ referred to as the query and key embeddings, respectively, then the attention weight can be represented as:

$$\alpha(\mathbf{x}, \mathbf{x}_i) = \text{softmax}(\mathbf{q}^T \mathbf{k}_i) = \frac{\exp(\mathbf{q}^T \mathbf{k}_i)}{\sum_{j=1}^n \exp(\mathbf{q}^T \mathbf{k}_j)}, \quad (5)$$

where \mathbf{W}_q and \mathbf{W}_k are matrices of parameters which are learned, for example, by incorporating an additional feed forward neural network within the system architecture.

Several attention weights defining the attention modules have been proposed for different applications. They can be divided into the additive attention [44] and multiplicative or dot-product attention [51, 52]. As pointed out by [53], the attention modules can be also classified as general attention, concat attention, and a location-based attention modules [51]. In particular, the general attention uses learnable parameters for keys and queries as it is illustrated in 5 (parameters \mathbf{W}_q and \mathbf{W}_k). The concat attention uses the concatenation of keys and queries. In the location-based attention, the scoring function depends only on queries and does not depend on keys. A list of common attention types can be found in [53].

4 The proposed method

Suppose that there are N bags X_1, \dots, X_N with labels Y_1, \dots, Y_N . Every bag consists of m_k patches or instances, $k = 1, \dots, N$.

Let us consider the main algorithm of using neighbors of each patch and learnable templates which can be regarded as a result of applying attention modules. A scheme of the algorithm is shown in Fig. 1.

Suppose we have N bags in the form of histological images. It should be noted that the histological application is taken to make a more clear illustration of the proposed algorithm. At the same time, we will study datasets different from the histological application in the same way by using this algorithm. Let us consider an image or a bag with the number of patches m . It is shown in Fig. 1 as the histological image. We consider the i -th and the j -th patches of the image which are highlighted in different colors.

All patches are fed to the input of a trained neural network (encoder or feature extractor) for computing their embedding F_i , i.e.,

$$F_i = \text{Conv}(I_i), \quad i = 1, \dots, m. \quad (6)$$

Embeddings F_i are produced to reduce the patch dimensionality.

For every patch, we also select a set of neighbors of adjacent patches. Let (x_i, y_i) and $\mathcal{M} = \{1, \dots, m\}$ be integer coordinates of the i -th patch in the whole image and the index set of all patches in the whole

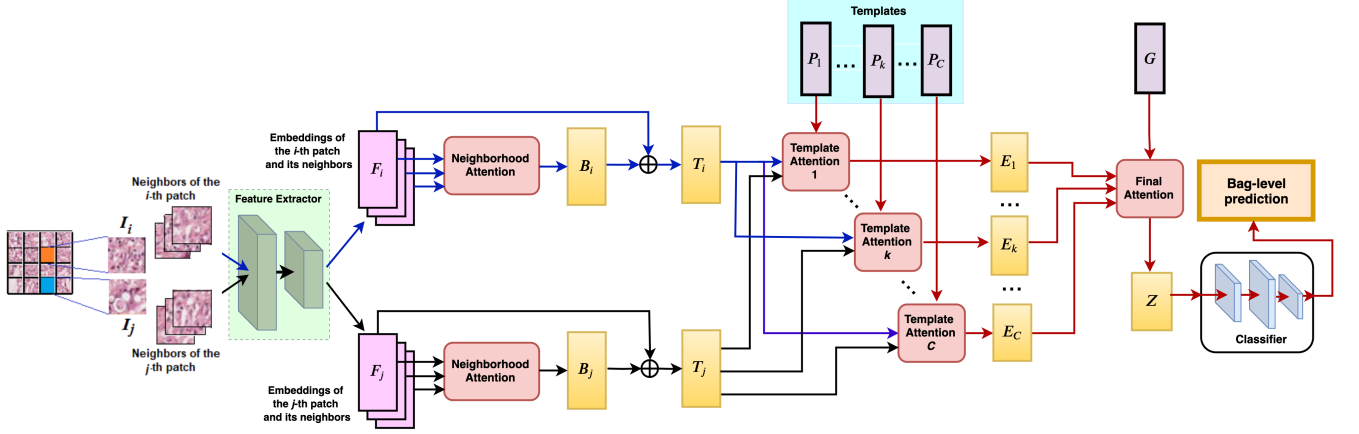


Figure 1: A scheme illustrating two paths of the patch processing in the neural network which implement the proposed algorithm

image, respectively. Then the index set $\mathcal{N}_i \subset \mathcal{M}$ of neighbors of the i -th patch is determined as

$$\mathcal{N}_i = \{j \in \mathcal{M} \mid 0 < \max(|x_i - x_j|, |y_i - y_j|) \leq d\}. \quad (7)$$

In our experiments the parameter d is taken equal to 1, but it can generally be arbitrary and depends on a size of patches. Moreover, other definitions of neighbors can be applied, for example, adjacent patches. The proposed algorithm depicted in Fig. 1 is general, and it is not restricted by a certain definition of neighbors. The idea to use the neighbor patches is based on the assumption that these patches may carry some useful information about a structure of the image. Moreover, the use of neighbors can be viewed as some kind of augmentation which may improve the classification results. Therefore, the next questions are how to take into account the patch neighbor information, how to perform identical neighbors of different patches, how to perform different numbers of neighbors. The answer is to use the attention mechanism. Namely, the joint embedding B_i of its neighbors with numbers from the index set \mathcal{N}_i of neighbors of the i -th patch is computed by means of the attention mechanism.

The embedding B_i of neighbors is determined as

$$B_i = \sum_{j \in \mathcal{N}_i} \alpha_j^{(i)} F_j. \quad (8)$$

Here weight $\alpha_j^{(i)}$ of the j -th neighbor is determined in accordance with relevance of the j -th patch embedding to vector F_i , i.e. it is determined in accordance with proximity of embedding F_j , $j \in \mathcal{N}_i$, of the corresponding neighbor patch to embedding F_i of the analyzed patch I_i . Hence, we use the original attention weights computed as follows:

$$\alpha_j^{(i)} = \text{softmax}(\mathbf{s}^{(i)}) = \frac{\exp(s_j^{(i)})}{\sum_t \exp(s_t^{(i)})}, \quad (9)$$

where $s_j^{(i)}$ is the attention scoring function that maps two vectors F_i and F_j to a scalar, i.e.,

$$s_j^{(i)} = \text{score}_{nb}(F_i, F_j). \quad (10)$$

It is defined in the proposed algorithm as

$$\text{score}_{nb}(F_i, F_j) = F_i^T \tanh(V_{nb} F_j), \quad (11)$$

where V is the matrix of learnable parameters.

In sum, we get a single embedding B_i for each F_i , which contains information about neighbors. It allows us to get joint embedding of the i -th patch embedding F_i and the embedding of neighbors. This can be done by means of concatenation of embeddings, i.e., the embedding of the i -th patch is concatenated with the joint embedding of neighbors B_i to get the patch embedding T_i with neighborhood as:

$$T_i = (F_i, B_i). \quad (12)$$

The concatenation operation is depicted in Fig. 1 by symbol \oplus . In fact, each bag is represented by the set of embeddings T_i now.

Another important concept proposed in the algorithm is a set of embedding templates which are regarded as learnable vectors. Moreover, the number of templates is the hyperparameter C whose value determines the quality of classification. Templates can be regarded as implementation of multiple attention applied to the set of embeddings T_i . They are different due to different initialization rules of the neural network.

Let us denote the set of templates as $\mathcal{P} = \{P_1, \dots, P_C\}$ and the k -th template as $P_k \in \mathcal{P}$. Then every template attention produces the corresponding aggregate embedding E_k which is computed as follows:

$$E_k = \sum_{i=1}^m \beta_i^{(k)} T_i, \quad k = 1, \dots, C, \quad (13)$$

where

$$\beta_i^{(k)} = \text{softmax}(\langle \text{score}(P_k, T_i) \rangle_i). \quad (14)$$

It can be seen from the above that the k -th aggregate embedding E_k is the weighted mean of all patch embeddings with neighborhood from an image with the weights defined by the k -th template. In other words, the k -th aggregate embedding characterizes the whole image or the bag with respect to the k -th template. Information about all patches and their neighbors is contained in C vectors E_1, \dots, E_C now.

Aggregate embeddings E_k corresponding to all C templates are grouped into the overall vector Z which corresponds to the whole image or the bag and all templates:

$$Z = \sum_{k=1}^C \gamma_k E_k, \quad (15)$$

where

$$\gamma_k = \text{softmax}(\langle \text{score}_{fin}(G, E_k) \rangle_k), \quad (16)$$

G is the global template as a training vector.

Template G and the corresponding final attention determine which aggregate embeddings E_k and templates P_k are important. The overall vector Z is a feature representation of the whole bag or the image, and it takes into account all peculiarities of the bag. It should be noted that we could aggregate E_1, \dots, E_C by using their concatenation. However, the aggregation of embeddings E_k by means of the final attention mechanism instead of their simple concatenation allows us to reduce the input dimension of the classifier, thereby increasing the generalization ability of the model and allowing possible training on small datasets. Moreover, the use of attention mechanism before the classifier leads to model interpretability, even if classifier is not interpretable.

It is proposed to use the classification layers $g_\theta(Z)$ with parameters θ , which defines the probability of class 1 at the bag level (the whole image level). In the simplest case, the layers are linear with the softmax,

but an arbitrary classification neural network can also be used. It is important that predictions can be interpreted even by using a complex neural network.

We have described one path of the i -th patch processing. Fig. 1 illustrates two paths corresponding to processing of the i -th and the j -th patches. However, the real implementation supposes to process all patches of a bag in the same way.

The whole neural network is trained end-to-end using the stochastic gradient descent and the Adam optimizer. At each step, an image (a bag) is selected from the training set, then it is divided into patches. The patches are used as input of the neural network. The result of using the neural network is an estimate of the probability of a class which means, for example, whether the image contains malignant cells or not. The loss function is determined based on the obtained estimate and the whole image label. To update the neural network weights, values of partial derivatives of the loss function are determined for each trained parameter using an automatic differentiation algorithm. Then the training parameter values are updated in a standard way.

Since templates play a role of different feature representations of each bag, then the corresponding vectors should be different. This implies that the standard loss function of the classification training is supplemented by the additional term which provides the difference of vectors P_k , $k = 1, \dots, C$. Then the loss function is of the form:

$$L = \frac{1}{N} \sum_{k=1}^N BCE(Y_k, f(X_k)) + \frac{2}{C(C-1)} \sum_{i < j} (P_i^T \cdot P_j)^2. \quad (17)$$

Here the first term is the standard binary cross-entropy (BCE) loss function; $f(X_k)$ is the output of the whole neural network. The second term in the loss function tries to make pairs of templates P_i and P_j as different as possible.

5 Computing the patch importance

Another interesting advantage of the proposed model and the implementing algorithm can be referred to the prediction interpretation or explanation. The problem is to explain which patches have the largest impact on the prediction of the bag class. It turns out that the proposed model provides the opportunity to answer this question due to specific structure of the model, namely, due to a connection between overall vector Z and the patch embeddings T_i , $i = 1, \dots, m$.

The overall embedding Z can be expressed through the weighted sum of embeddings corresponding to patches. This follows from the following:

$$\begin{aligned} Z &= \sum_{k=1}^C \gamma_k E_k = \sum_{k=1}^C \gamma_k \left(\sum_{i=1}^m \beta_i^{(k)} T_i \right) \\ &= \sum_{i=1}^m \left(\sum_{k=1}^C \gamma_k \beta_i^{(k)} \right) T_i = \sum_{i=1}^m w_i T_i. \end{aligned} \quad (18)$$

Here weight $w_i = \sum_{k=1}^C \gamma_k \beta_i^{(k)}$ can be regarded as the *importance* of the i -th patch with its neighborhood. It is easy to show that there holds $\sum_{i=1}^m w_i = 1$.

It should be noted that the importance of the i -th patch neighbors is determined as $\alpha_j^{(i)}$ (see (8) and (9)). Hence, we can state the question how to connect the *importance* of the embedding T_i taking into account neighbors with the importance of patch F_i itself. If we assume that all elements of vector T_i are equivalent, then importance measures of its two parts are equal. However, B_i may depend on T_j if patches with indices i and j are neighbor. This implies that the final importance v_i of the i -th patch is determined as

$$v_i = w_i + \sum_{j \in N_i} \alpha_j^{(i)} w_j. \quad (19)$$

6 Again about templates

The proposed templates have several advantages which are discussed below.

First of all, templates can be used for classification of types of instances. This can be done by means of determining weights of the templates γ_k for a particular image (see (15) and (16)). Having a small dataset with labels in the form of types of instances (not binary), we can train a simple classifier that matches the vector $(\gamma_1, \dots, \gamma_C)$ with the type of instances.

Another advantage is a simple possibility of adding new templates or excluding unnecessary templates. Since the number of templates can be different without changing the network weights, templates can be added or excluded after training. Adding new templates corresponds to a scenario of appearance of a new type of cells (the encoder has to be able to construct informative embedding in this case). A new trainable vector of the template is added, and all other network parameters are not trained and remain without changes. The exclusion of templates can be carried out based on the statistics of template weights over the entire dataset. Templates with the lowest total weight can be excluded without reducing the prediction quality.

Templates can be visualized. For each template P_k , we can calculate its proximity to all patch embeddings T_i with neighborhoods of all dataset images and find the patch with the largest value of score (P_k, T_i) . This patch can be regarded as an approximate visualization of the template. An autoencoder reconstructing a patch image from its embedding can be trained such that the patch image reconstructed from a template can be viewed as the visualization of the template.

7 Numerical experiments

7.1 Datasets for experiments

We consider several dataset in order to study the proposed model.

First, we study the proposed model by applying the MNIST dataset which is a commonly used large dataset of 28x28 pixel handwritten digit images [30]. It has a training set of 60,000 instances, and a test set of 10,000 instances. The digits are size-normalized and centered in a fixed-size image. The dataset is available at <http://yann.lecun.com/exdb/mnist/>.

To study how neighbors and templates impact on predictions, we perform four datasets based on MNIST.

The first dataset called MNIST-MIL consists of groups (bags) of digits from MNIST of random size from 6 to 12 digits in a bag such that the bag label is 1 if there is at least one digit “9” among all digits in the bag, otherwise label 0 is assigned to the bag.

The second dataset called MNIST-MIL-1 consists of groups (bags) of digits from MNIST, which are composed similarly to the previous MNIST dataset, but label 1 is assigned to a bag if there is at least one pair of neighboring digits “9” and “3” in the arbitrary order, otherwise label 0 is assigned to the bag.

In the third dataset called MNIST-MIL-2, bags are formed in the same way as in MNIST-MIL-1, but label 1 is assigned to a bag if there is at least one digit “9”, which does not have neighbor “3” (on the left or on the right), otherwise label 0 is assigned to the bag.

The fourth dataset called MNIST-MIL-3 consists of groups (bags) of digits from MNIST, which are composed similarly to MNIST-MIL-2, but label 1 is assigned to a bag if there is at least one digit “9”, which does not have neighbor “3”, and there is at least one digit “7”, which does not have neighbor “4”, otherwise label 0 is assigned to the bag.

We also use datasets Musk1, Musk2 (drug activity) [1], Fox, Tiger, Elephant [16] with numerical features to study how the proposed method performs tabular data.

The Musk1 dataset contains 92 bags consisting of 476 instances with 166 features. The average bag size is 5.17. The Musk2 dataset contains 102 bags consisting of 6598 instances with 166 features. The average bag size is 64.69. Each dataset (Fox, Tiger and Elephant) contains exactly 200 bags consisting of

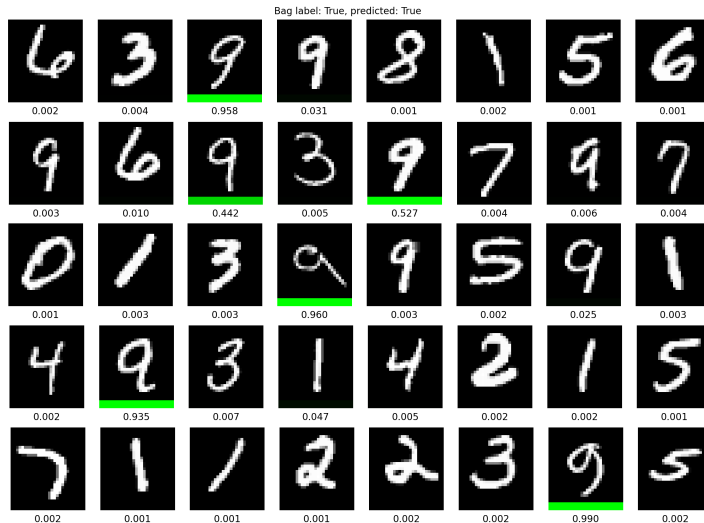


Figure 2: Examples of testing bags from MNIST-MIL-1, which belong to the true positive subset

instances with 230 features. Numbers of instances in datasets Fox, Tiger and Elephant are 1302, 1220 and 1391, respectively. The average bag sizes of the datasets are 6.60, 6.96 and 6.10, respectively.

In order to study the histology application of the proposed model and to compare this model with results obtained in [29], we use the Breast Cancer Cell Segmentation dataset [31] which consists of 58 histopathology images with expert annotations. Images are used in breast cancer cell detection with associated ground truth data available. The dataset aims to validate methods for cell segmentation and their classification. The dataset can be downloaded from <https://www.kaggle.com/andrewmvd/breast-cancer-cell-segmentation>.

Each image from the Breast Cancer Cell Segmentation dataset has the size 896×768 pixels and is divided into 672 non-intersecting patches of size 32×32 . Patches consisting of larger than 75% of white pixels are excluded from the dataset.

7.2 MNIST-MIL results

First, we study the proposed model trained on the dataset MNIST-MIL-1. Randomly selected bags are grouped in accordance with their class and the predicted class of the bag. The class of a bag in MNIST-MIL-1 is defined by existence of neighboring digits “9” and “3”. In order to correctly compare our experiments with AbDMIL [29], we use the same model (LeNet5 [30]) for training encoder depicted in Fig. 1 as “Feature Extractor” whose output is F_i as it is used in [29]. Parameters of the neural network and its training are shown in Tables 8-10 (see Appendix of [29]). In addition to the above, we use $C = 10$ templates for producing aggregate embeddings E_k . All embeddings F_i and B_i have the dimensionality which is equal to 128. Embeddings T_i , templates P_i , aggregate embeddings E_k , vectors G and Z are of size 256.

The first subset of five randomly selected testing bags is shown in Fig. 2. Every bag belongs to class 1 (true) because it has neighboring digits “9” and “3”. We take digits “9” and “3” because they can be mistaken with many digits, for example, with “5”, “4”, “2”, “8”. The algorithm successfully recognizes bags as elements of class 1 because it finds digit “9” with neighbor “3” in every bag. The importance v_i of patches (digits) are shown under the patches. It can be seen from Fig. 2 that digit “9” has the largest value of v_i .

Another case is depicted in Fig. 3 where examples of testing bags, which belong to the false negative

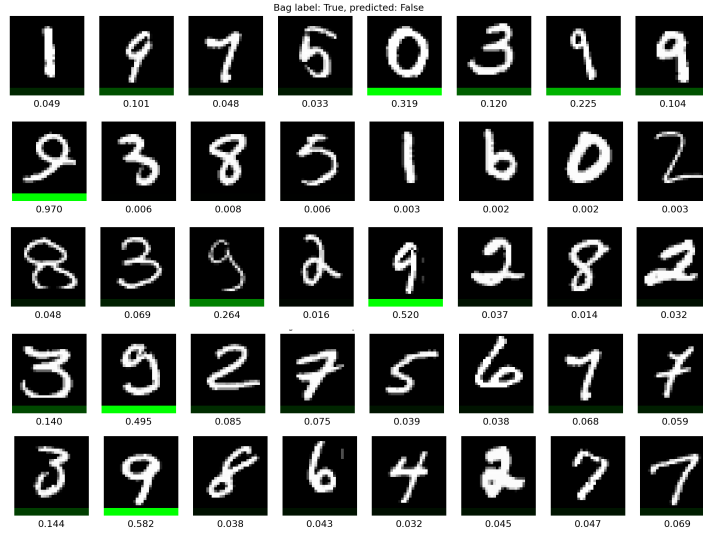


Figure 3: Examples of testing bags from MNIST-MIL-1, which belong to the false negative subset

subset, are shown. One can see from 3 that every bag contains a pair of adjacent digits “9” and “3” and can be regarded as belonging to class 1, but the classification model incorrectly classifies digits “9” as different digits or as “9” but with a adjacent digit different from “3”.

Fig. 4 illustrates cases of false positive examples when bags belong to class 0 because there are no adjacent pairs of digits “9” and “3”. It is interesting to note that the model recognizes digits akin to “9” as “9” with adjacent “3”. For example, digit “5” in the first bag is akin to “9”, and there is digit “3” on the left. However, this is an incorrect prediction. In other words, the model correctly looks for the pair “9” and “3” and fails due to the incorrect classification of “9”.

The last case of classification based on MNIST-MIL-1 is shown in Fig. 5 where bags belong to class 0 because there are no adjacent digits “9” and “3”, and the model successfully classifies the bags as negative. One can see from Fig. 5 that the model correctly recognizes “9” in all cases except for the second bag, but the recognized digits do not have adjacent “3”. In the second bag, the model has detected the adjacent pair “3” and “9”, but it incorrectly classifies the second digit as “9”.

Let us consider the proposed model trained on the dataset MNIST-MIL-2. Randomly selected bags are grouped in accordance with their class and the predicted class of the bag. The class of a bag in MNIST-MIL-2 is defined by existence at least one digit “9” without adjacent digit “3”.

The first subset of five randomly selected testing bags is shown in Fig. 6. Every bag belongs to class 1 (true) because it has neighboring digits “9” and “3”. The algorithm successfully recognizes bags as elements of class 1 because it finds digit “9” with neighbor “3” in every bag. The importance v_i of patches (digits) are shown under every patch image. It can be seen from Fig. 6 that digit “9” has the largest value of v_i . At that, all classified digits “9” do not have neighbor digits “3”.

Fig. 7 illustrates another case when examples of testing bags, which belong to the true negative subset, are shown. One can see from 7 that every bag contains digits “9” without adjacent digits “3”, i.e., the bags belong to class 1. However, the classifier incorrectly recognizes digits “9”.

The false positive examples, when bags belong to class 0 because there are no digits “9” in the bags, are depicted in Fig. 8. The classifier incorrectly recognizes digits “4” as “9” which do not have adjacent digits “3”.

Examples from the true negative subset of MNIST-MIL-2 are shown in Fig. 9. Bags do not have digits “9” and the classifier does not find these digits.

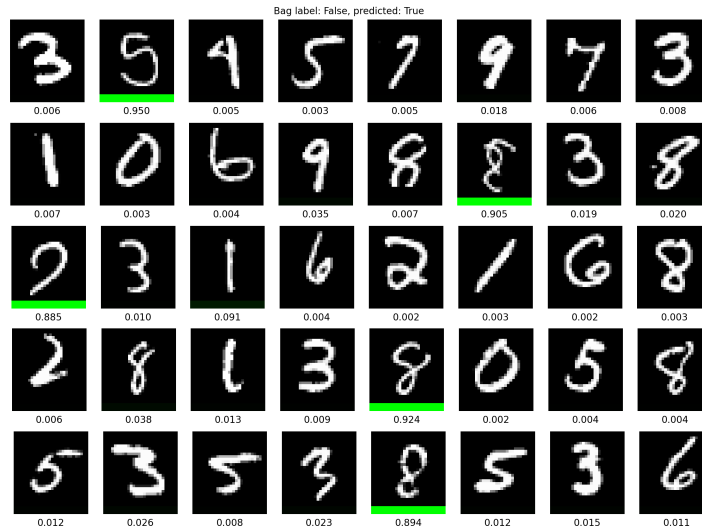


Figure 4: Examples of testing bags from MNIST-MIL-1, which belong to the false positive subset

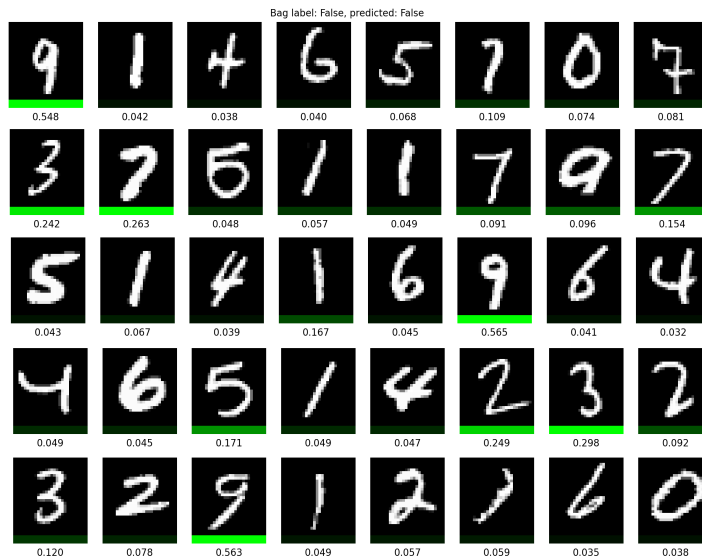


Figure 5: Examples of testing bags from MNIST-MIL-1, which belong to the true negative subset

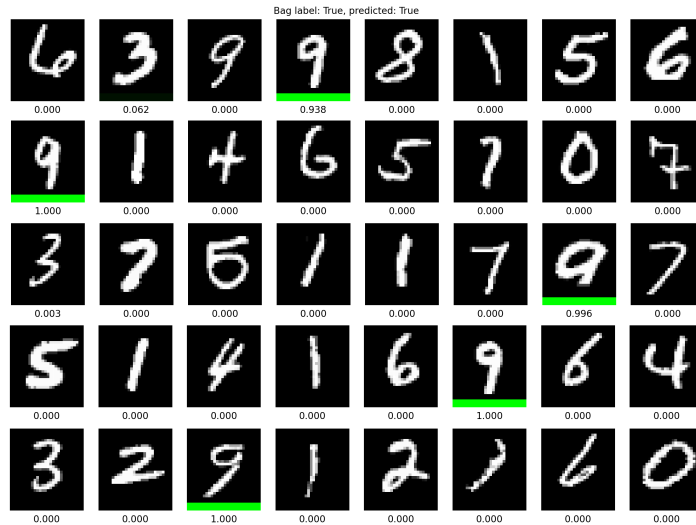


Figure 6: Examples of testing bags from MNIST-MIL-2, which belong to the true positive subset

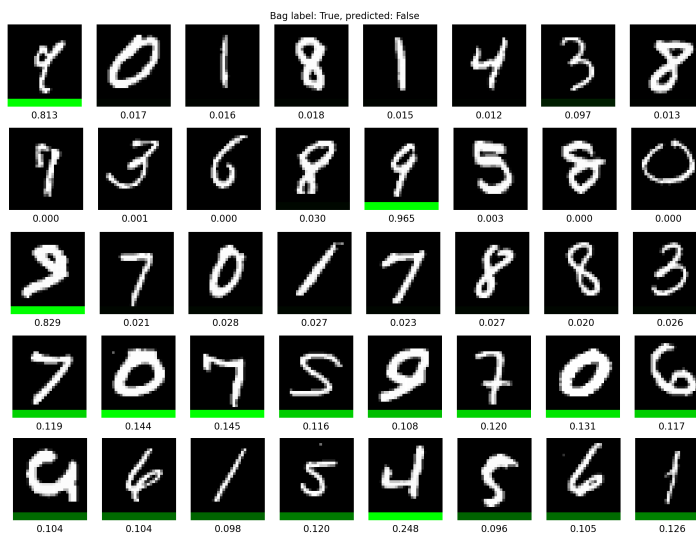


Figure 7: Examples of testing bags from MNIST-MIL-2, which belong to the true negative subset

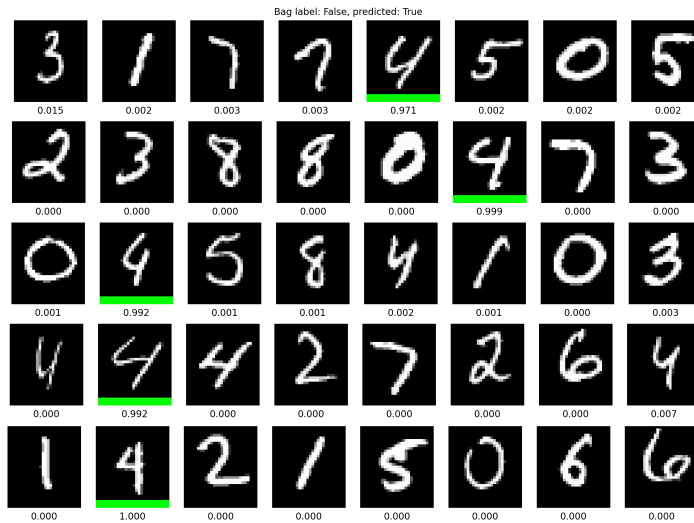


Figure 8: Examples of testing bags from MNIST-MIL-2, which belong to the false positive subset

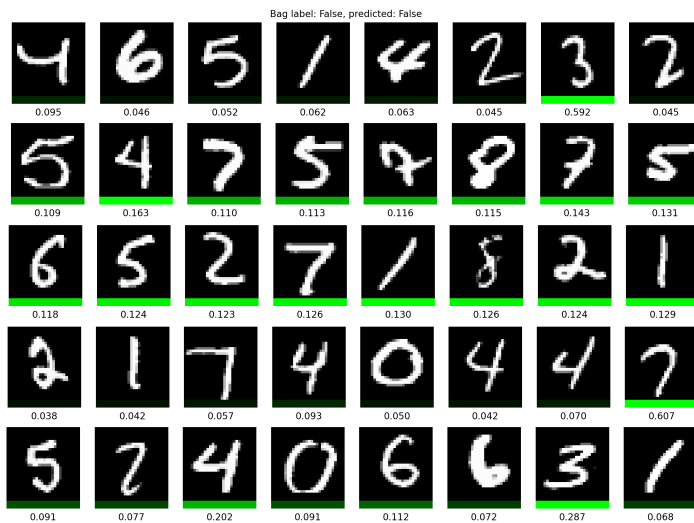


Figure 9: Examples of testing bags from MNIST-MIL-2, which belong to the true negative subset

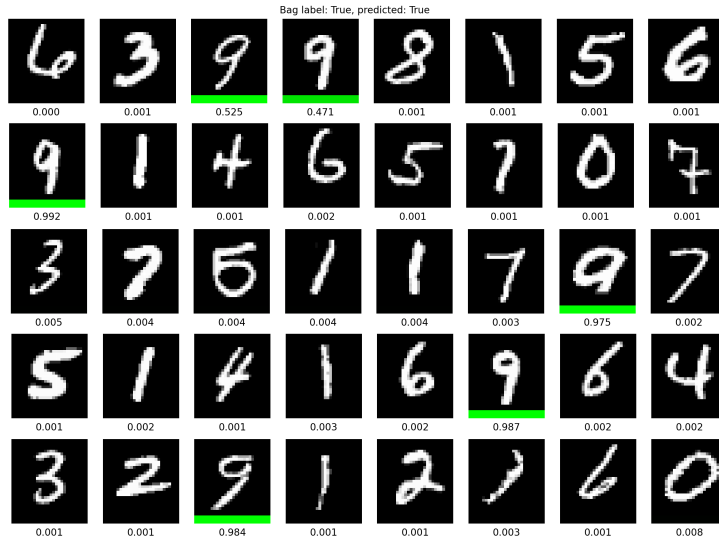


Figure 10: Examples of testing bags from MNIST-MIL, which belong to the true positive subset

Table 1: The accuracy and F1 measures for models AbDMIL and MAMIL trained on different datasets formed from MNIST

Datasets	Method	Accuracy	F1
MNIST-MIL-1	AbDMIL	0.806	0.581
MNIST-MIL-1	MAMIL	0.987	0.945
MNIST-MIL-2	AbDMIL	0.909	0.910
MNIST-MIL-2	MAMIL	0.980	0.979
MNIST-MIL-3	AbDMIL	0.874	0.601
MNIST-MIL-3	MAMIL	0.866	0.913
MNIST-MIL	AbDMIL	0.973	0.976
MNIST-MIL	MAMIL	0.983	0.985

Similar examples of bags from MNIST-MIL dataset are shown in Figs. 10-13. Classes of bags are defined by the simplest condition when digit “9” is available in the bag.

The classification accuracy and F1 measure of the proposed model MAMIL and the attention MIL [29] are given in Table 1. It can be seen from Table 1 that MAMIL outperforms AbDMIL for all dataset. The F1 measure is used for comparison and analyzing the models because all dataset are imbalanced. It is interesting to conclude from the numerical results that MAMIL significantly outperforms AbDMIL for datasets with complex conditions of classes. In particular, the dataset MNIST-MIL-3 has the most restrictive condition (digit “9” without neighbor “3” and digit “7” without neighbor “4”), and the difference between F1 measures for MAMIL and AbDMIL, respectively, is 0.312.

To study how the number of templates impacts on the accuracy measure, we consider the most interesting case of the MNIST-MIL-3 dataset. Fig. 14 shows how the F1 measure depends on parameter C . It is interesting to observe that there is some optimal values ($C = 6$ for the considered case) of the template number which provides the largest value of accuracy. However, the optimal value of C can be found only by its enumerating in some interval if the number of types of patches is unknown.

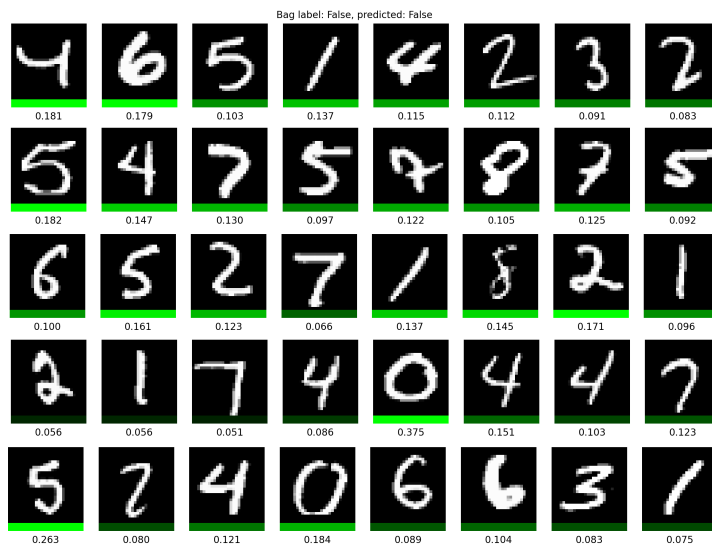


Figure 11: Examples of testing bags from MNIST-MIL, which belong to the false negative subset



Figure 12: Examples of testing bags from MNIST-MIL, which belong to the false positive subset

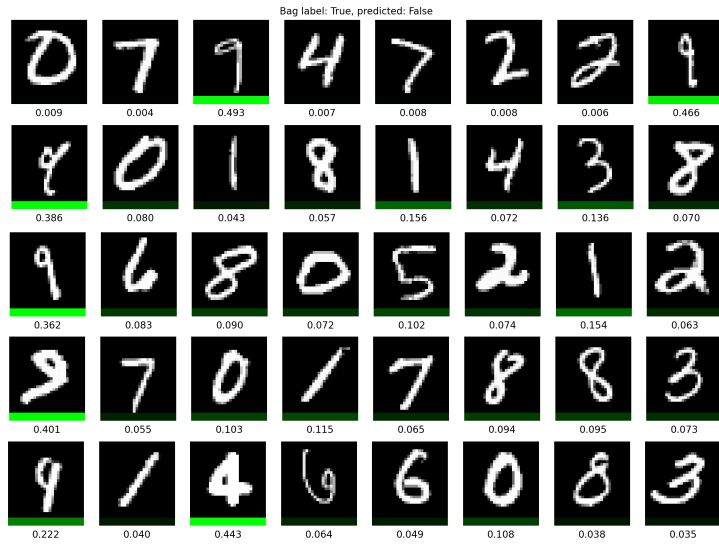


Figure 13: Examples of testing bags from MNIST-MIL, which belong to the true negative subset

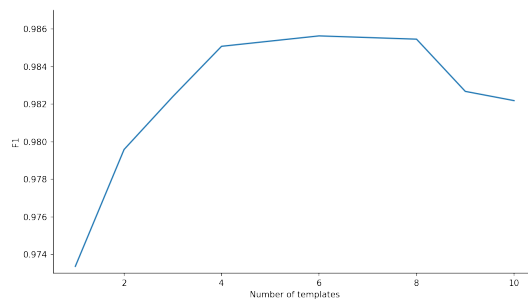


Figure 14: The F1 measure as a function of parameter C (the number of templates)

Table 2: The accuracy measures for AbDMIL and MAMIL trained on datasets Musk1, Musk2, Fox, Tiger, Elephant

	AbDMIL	Loss-Attention	MAMIL
Musk1	0.900	0.917	0.912
Musk2	0.863	0.911	0.927
Fox	0.615	0.712	0.844
Tiger	0.845	0.897	0.902
Elephant	0.868	0.900	0.906

7.3 Datasets Musk1, Musk2, Fox, Tiger, Elephant

In order to compare MAMIL and the AbDMIL models, we also train the corresponding models on well-known datasets Musk1, Musk2, Fox, Tiger, Elephant. It is important to point out that the AbDMIL prediction accuracy measures are obtained for these datasets in [29]. Moreover, they are compared with many available MIL models, including mi-SVM [16], MI-SVM [16], MI-Kernel[54], EM-DD [55], mi-Graph [56], miVLAD [57], miFV [57], mi-Net [20], MI-Net [20], MI-Net with DS [20], MI-Net with RC [20]. The corresponding results can be found in Table 1, Subsection 4.1 in [29]. Therefore, we compare MAMIL only with the AbDMIL [29] to demonstrate its properties. To consider the AbDMIL method, we take the best accuracy measure among Attention and Gated-Attention methods.

In our experiments we use the same architecture, optimizer and hyperparameters of the first Feature Extractor as in the Attention-MIL [29]. Other parameters are the same as in the experiments with MNIST, i.e., $C = 10$, all embeddings F_i have the dimensionality which is equal to 128, embeddings T_i , templates P_i , aggregate embeddings E_k , vectors G and Z are of the same size 128. It should be pointed out that the whole model is trained without using neighbors because they are not correlated and may worsen the prediction results. In contrast to the image datasets, the considered tabular datasets do not have any adjacency relations, i.e., neighbors of instances are not defined. However, Table 2 illustrates that use of multiple attention modules allows us to significantly enhance the classification accuracy. One can see from Table 2 that MAMIL outperforms AbDMIL for all considered datasets.

We also add for comparison purposes the results available for the Loss-Attention MIL method [24] based on the same datasets. which provide slightly better results in comparison with AbDMIL. It can be seen from Table 2 that the Loss-Attention method outperforms MAMIL only for Musk1. However, MAMIL shows better predictions for other datasets.

7.4 Breast Cancer results

Fig. 15 illustrates examples of histology images from the Breast Cancer Cell Segmentation dataset divided into patches (the first column), heatmaps created in accordance with weights of patches with images (the second column), ground truth: patches that belong to class 1 (the third column). To perform experiments with the Breast Cancer dataset, we use $C = 10$ templates for producing aggregate embeddings E_k . All embeddings F_i and B_i have the dimensionality which is equal to 128. Embeddings T_i , templates P_i , aggregate embeddings E_k , vectors G and Z are of size 256. Heatmaps are computed by using (18)-(19). One can see from Fig. 15 that there is a matching between the heatmaps and the ground truth. Moreover, the bag classification accuracy for the training regime is 0.968 whereas for the testing regime is 0.917.

8 Conclusion

A new model for solving the MIL problem by using the multiple attention mechanism has been proposed. It differs from many models by several peculiarities. First, it takes into account neighbors of each instance from a bag. Second, it uses a specific scheme in the form of the neighborhood attention for joining the

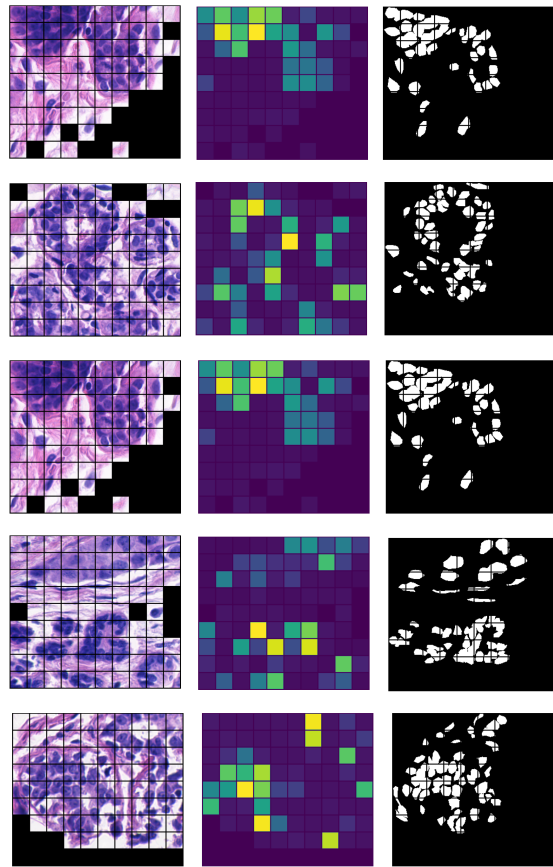


Figure 15: Examples of histology images from the Breast Cancer Cell Segmentation dataset (the first column), heatmaps constructed in accordance with weights of patches with images (the second column), ground truth: patches that belong to class 1 (the third column).

instance and its neighbor information. Third, it uses a set of attention operations to join information from all instances and its neighbors in the bag. Fourth, it directly explains results of classification.

Numerical experiments have demonstrated that MAMIL is comparable with the Loss-Attention model [24] and the AbDMIL model [29] and outperforms for most datasets analyzed. In contrast to these models, MAMIL is more flexible because a proper choice of numbers of templates and neighbors may significantly improve the model.

MAMIL is not only flexible, but it is rather general and has several elements which can be changed. First, the concatenation operation is used to unite embeddings of a patch and its neighbors. However, this operation can be replaced with the weighted sum of the corresponding embedding vectors like the attention scheme. Moreover, parameters of the attention can be trainable. This replacement may compensate anomalous “mean” neighborhood embeddings and reduce the dimensionality of joint embeddings. Another interesting direction for the model modification is extend the proposed scheme to the neighboring bags. The idea is that neighboring bags from a dataset like neighboring instances may also improve the classification properties. In other words, the proposed scheme of multiple attention modules can be extended to the level of bags. Moreover, it is interesting to consider a case of unlabeled bags, i.e., to consider the self-supervised learning model with clusterization. The above ideas can be regarded as interesting directions for further research.

Acknowledgement

This work is supported by the Russian Science Foundation under grant 21-11-00116.

References

- [1] T.G. Dietterich, R.H. Lathrop, and T. Lozano-Perez. Solving the multiple instance problem with axis-parallel rectangles. *Artificial Intelligence*, 89:31–71, 1997.
- [2] L. Zhu, B. Zhao, and Y. Gao. Multi-class multi-instance learning for lung cancer image classification based on bag feature selection. In *2008 Fifth International Conference on Fuzzy Systems and Knowledge Discovery*, volume 2, pages 487–492. IEEE, 2008.
- [3] X.-S. Wei, H.-J. Ye, X. Mu, J. Wu, C. Shen, and Z.-H. Zhou. Multiple instance learning with emerging novel class. *IEEE Transactions on Knowledge and Data Engineering*, 33(5), 2019.
- [4] M. Hagele, P. Seegerer, S. Lapuschkin, M. Bockmayr, W. Samek, F. Klauschen, K.-R. Muller, and A. Binder. Resolving challenges in deep learning-based analyses of histopathological images using explanation methods. *Scientific Report*, 10(6423):1–12, 2020.
- [5] J. van der Laak, G. Litjens, and F. Ciompi. Deep learning in histopathology: the path to the clinic. *Nature Medicine*, 27:775–784, 2021.
- [6] Y. Yamamoto, T. Tsuzuki, and J. Akatsuka. Automated acquisition of explainable knowledge from unannotated histopathology images. *Nature Communications*, 10(5642):1–9, 2019.
- [7] J. Amores. Multiple instance classification: review, taxonomy and comparative study. *Artificial Intelligence*, 201:81–105, 2013.
- [8] B. Babenko. Multiple instance learning: Algorithms and applications. Technical report, University of California, San Diego, 2008.
- [9] M.-A. Carbonneau, V. Cheplygina, E. Granger, and G. Gagnon. Multiple instance learning: A survey of problem characteristics and applications. *Pattern Recognition*, 77:329–353, 2018.

- [10] V. Cheplygina, M. de Bruijne, and J.P.W. Pluim. Not-so-supervised: A survey of semi-supervised, multi-instance, and transfer learning in medical image analysis. *Medical Image Analysis*, 54:280–296, 2019.
- [11] G. Quellec, G. Cazuguel, B. Cochener, and M. Lamard. Multiple-instance learning for medical image and video analysis. *IEEE Reviews in Biomedical Engineering*, 10:213–234, 2017.
- [12] J. Yao, X. Zhu, J. Jonnagaddala, N. Hawkins, and J. Huang. Whole slide images based cancer survival prediction using attention guided deep multiple instance learning network. *Medical Image Analysis*, 65(101789):1–14, 2020.
- [13] Z.-H. Zhou. Multi-instance learning: A survey. Technical report, National Laboratory for Novel Software Technology, Nanjing University, 2004.
- [14] C.L. Srinidhi, O. Ciga, and A.L.Martel. Deep neural network models for computational histopathology: A survey. *Medical Image Analysis Volume 67, January 2021, 101813*, 67:101813, 2021.
- [15] J. Wang and J.-D. Zucker. Solving the multiple-instance problem: A lazy learning approach. In *Proceedings of the seventeenth international conference on machine learning, ICML*, pages 1119–1126, 2000.
- [16] S. Andrews, I. Tsochantaridis, and T. Hofmann. Support vector machines for multiple-instance learning. In *Proceedings of the 15th international conference on neural information processing systems, NIPS’02*, pages 577–584. MIT Press, Cambridge, MA, USA, 2002.
- [17] Y. Chevaleyre and J.-D. Zucker. Solving multiple-instance and multiple-part learning problems with decision trees and rule sets. application to the mutagenesis problem. In *Biennial Conference of the Canadian Society on Computational Studies of Intelligence: Advances in Artificial Intelligence*, volume 2056 of *Lecture Notes in Computer Science*, pages 204–214. Springer, Berlin, Heidelberg, 2001.
- [18] O.Z. Kraus, J.L. Ba, and B.J. Frey. Classifying and segmenting microscopy images with deep multiple instance learning. *Bioinformatics*, 32(12):i52–i59, 2016.
- [19] M. Sun, T.X. Han, M.-C. Liu, and A. Khodayari-Rostamabad. Multiple instance learning convolutional neural networks for object recognition. In *International conference on pattern recognition (ICPR)*, pages 3270–3275, 2016.
- [20] X. Wang, Y. Yan, P. Tang, X. Bai, and W. Liu. Revisiting multiple instance neural networks. *Pattern Recognition*, 74:15–24, 2018.
- [21] N. Pappas and A. Popescu-Belis. Explicit document modeling through weighted multiple-instance learning. *Journal of Artificial Intelligence Research*, 58:591–626, 2017.
- [22] D. Rymarczyk, A. Kaczynska, J. Kraus, A. Pardył, and B. Zielinski. ProtoMIL: Multiple instance learning with prototypical parts for fine-grained interpretability. arXiv:2108.10612, Aug 2021.
- [23] S. Jiang, A. Suriawinata, and S. Hassanpour. Mhattsurv: Multi-head attention for survival prediction using whole-slide pathology images. arXiv: 2110.11558, Oct 2021.
- [24] X. Shi, F. Xing, Y. Xie, Z. Zhang, L. Cui, and L. Yang. Loss-based attention for deep multiple instance learning. In *Proceedings of the AAAI Conference on Artificial Intelligence*, volume 34, pages 5742–5749, 2020.
- [25] X. Tang, M. Liu, H. Zhong, Y. Ju, W. Li, and Q. Xu. MILL: Channel attention-based deep multiple instance learning for landslide recognition. *ACM Transactions on Multimedia Computing, Communications, and Applications (TOMM)*, 17(2s):1–11, 2021.

- [26] S. Fuster, T. Eftestol, and K. Engan. Nested multiple instance learning with attention mechanisms. arXiv:2111.00947, Nov 2021.
- [27] B. Li, Y. Li, and K.W. Eliceiri. Dual-stream multiple instance learning network for whole slide image classification with self-supervised contrastive learning. In *Proceedings of the IEEE/CVF Conference on Computer Vision and Pattern Recognition*, pages 14318–14328, 2021.
- [28] Q. Wang, Y. Zhou, J. Huang, Z. Liu, L. Li, W. Xu, and J.-Z. Cheng. Hierarchical attention-based multiple instance learning network for patient-level lung cancer diagnosis. In *2020 IEEE International Conference on Bioinformatics and Biomedicine (BIBM)*, pages 1156–1160. IEEE, 2020.
- [29] M. Ilse, J. Tomczak, and M. Welling. Attention-based deep multiple instance learning. In *Proceedings of the 35th International Conference on Machine Learning, PMLR*, volume 80, pages 2127–2136, 2018.
- [30] Y. LeCun, L. Bottou, Y. Bengio, and P. Haffner. Gradient-based learning applied to document recognition. *Proceedings of the IEEE*, 86(11):2278–2324, 1998.
- [31] E.D. Gelasca, J. Byun, B. Obara, and B.S. Manjunath. Evaluation and benchmark for biological image segmentation. In *IEEE International Conference on Image Processing*, pages 1816–1819. IEEE, Oct 2008.
- [32] P. Auer and R. Ortner. A boosting approach to multiple instance learning. In *European Conference on Machine Learning*, pages 63–74. Springer, Berlin, Heidelberg, 2004.
- [33] C. Leistner, A. Saffari, and H. Bischof. Miforests: Multiple-instance learning with randomized trees. In *European Conference on Computer Vision*, pages 29–42. Springer, Berlin, Heidelberg, 2010.
- [34] S. Mei and H. Zhu. Adaboost based multi-instance transfer learning for predicting proteome-wide interactions between Salmonella and human proteins. *PLoS One*, 9(10):e110488, 2014.
- [35] P.Y. Taser, K.U. Birant, and D. Birant. Comparison of ensemble-based multiple instance learning approaches. In *2019 IEEE International Symposium on INnovations in Intelligent SysTems and Applications (INISTA)*, pages 1–5, 2019.
- [36] G. Doran and S. Ray. Multiple-instance learning from distributions. *Journal of Machine Learning Research*, 17:1–50, 2016.
- [37] Y.Y. Xu. Multiple-instance learning based decision neural networks for image retrieval and classification. *Neurocomputing*, 171:826–836, 2016.
- [38] J. Feng and Z.-H. Zhou. Deep miml network. In *Proceedings of the AAAI Conference on Artificial Intelligence*, volume 31, pages 1884–1890, 2017.
- [39] Q. Liu, S. Zhou, C. Zhu, X. Liu, and J. Yin. MI-ELM: Highly efficient multi-instance learning based on hierarchical extreme learning machine. *Neurocomputing*, 173(3):1044–1053, 2016.
- [40] A.B. Arrieta, N. Diaz-Rodriguez, J. Del Ser, A. Bennetot, S. Tabik, A. Barbado, S. Garcia, S. Gil-Lopez, D. Molina, R. Benjamins, R. Chatila, and F. Herrera. Explainable artificial intelligence (XAI): Concepts, taxonomies, opportunities and challenges toward responsible AI. *Information Fusion*, 58:82–115, 2020.
- [41] R. Guidotti, A. Monreale, D. Pedreschi, and F. Giannotti. Principles of explainable artificial intelligence. In *Explainable AI Within the Digital Transformation and Cyber Physical Systems*, pages 9–31. Springer, Cham, 2021.
- [42] X. Li, H. Xiong, X. Li, X. Wu, X. Zhang, J. Liu, J. Bian, and D. Dou. Interpretable deep learning: Interpretations, interpretability, trustworthiness, and beyond. arXiv:2103.10689, Mar 2021.

- [43] C. Rudin, C. Chen, Z. Chen, H. Huang, L. Semenova, and C. Zhong. Interpretable machine learning: Fundamental principles and 10 grand challenges. arXiv:2103.11251, March 2021.
- [44] D. Bahdanau, K. Cho, and Y. Bengio. Neural machine translation by jointly learning to align and translate. arXiv:1409.0473, Sep 2014.
- [45] A. Zhang, Z.C. Lipton, M. Li, and A.J. Smola. Dive into deep learning. arXiv:2106.11342, Jun 2021.
- [46] D. Rymarczyk, A. Borowa, J. Tabor, and B. Zielinski. Kernel self-attention for weakly-supervised image classification using deep multiple instance learning. In *IEEE Winter Conference on Applications of Computer Vision (WACV)*, pages 1721–1730. IEEE, 2021.
- [47] C.R. Qi, S. Hao, M. Kaichun, and J.G. Leonidas. Pointnet: Deep learning on point sets for 3d classification and segmentation. In *Proceedings of the IEEE conference on computer vision and pattern recognition*, pages 652–660, 2017.
- [48] S. Chaudhari, V. Mithal, G. Polatkan, and R. Ramanath. An attentive survey of attention models. arXiv:1904.02874, Apr 2019.
- [49] E.A. Nadaraya. On estimating regression. *Theory of Probability & Its Applications*, 9(1):141–142, 1964.
- [50] G.S. Watson. Smooth regression analysis. *Sankhya: The Indian Journal of Statistics, Series A*, pages 359–372, 1964.
- [51] T. Luong, H. Pham, and C.D. Manning. Effective approaches to attention-based neural machine translation. In *Proceedings of the 2015 Conference on Empirical Methods in Natural Language Processing*, pages 1412–1421. The Association for Computational Linguistics, 2015.
- [52] A. Vaswani, N. Shazeer, N. Parmar, J. Uszkoreit, L. Jones, A.N. Gomez, L. Kaiser, and I. Polosukhin. Attention is all you need. In *Advances in neural information processing systems*, pages 5998–6008, 2017, 2017.
- [53] Z. Niu, G. Zhong, and H. Yu. A review on the attention mechanism of deep learning. *Neurocomputing*, 452:48–62, 2021.
- [54] T. Gartner, P.A. Flach, A. Kowalczyk, and A.J. Smola. Multi-instance kernels. In *Proceedings of ICML*, volume 2, pages 179–186, 2002.
- [55] Q. Zhang and S.A. Goldman. Em-dd: An improved multiple-instance learning technique. In *Proceedings of NIPS*, pages 1073–1080, 2002.
- [56] Z.-H. Zhou, Y.-Y. Sun, and Y.-F. Li. Multi-instance learning by treating instances as non-iid samples. In *Proceedings of ICML*, pages 1249–1256, 2009.
- [57] X.-S. Wei, J. Wu, and Z.-H. Zhou. Scalable algorithms for multi-instance learning. *IEEE Transactions on Neural Networks and Learning Systems*, 28(4):975–987, 2017.